Correspondence

Three-Dimensional Imaging Using a New Synthetic Aperture Focusing Technique

Ahmed Yamani, *Senior Member, IEEE*

***Abstract*—The drawbacks of the multifrequency automatic focusing technique (MF-AFT) have been eased considerably when the scanned-frequency signals are transmitted simultaneously in a pulse. While the focusing capabilities of the MF-AFT are maintained, substantial reduction in data processing is obtained when the new procedure is used. In addition, the derived pulse can be tailored to further enhance the quality of the image produced by this new procedure. Simulation results are included to demonstrate the focusing capabilities of the procedure for both two- and three-dimensional objects.**

I. Introduction

ULTRASONIC NONDESTRUCTIVE TESTING (NDT) has recently been required not only to detect defects inside components and devices with high resolution, but also to characterize the detected flaws by their size, shape, orientation, and location so that rational decisions about the safe operation of these components can be made. Ultrasonic imaging has become a valuable inspection tool, and thus is required to be very powerful to accomplish this objective.

An important feature of any imaging system concerns its ability to unambiguously resolve the details of a target. In general, resolution and ambiguity can be governed by a suitable choice of the collecting aperture size, its shape, and the effective weighting function applied as the target information is recorded and processed to produce an image. However, for a given set of focusing conditions, these properties can only be maintained over a limited region of image space, which is usually known as the depth of field or depth of focus (DOF) [1]. Beyond this region, image degradation becomes unacceptable. The synthetic aperture focusing technique (SAFT) [2]–[6] has long been recognized as a method well suited for generating high resolution images over a large (compared to the wavelength) DOF. The original SAFT approach, which made use of a time-delay algorithm for simulating the required lens effect, has nowadays been implemented upon specially designed real-time SAFT processors [4] and has been used to produce 3-dimensional images. However, in several applications such as medical imaging and NDT, the target to be imaged can be located in the close near field of the data collection aperture where the DOF is particularly small and leads to difficulties in image interpretation.

It has been demonstrated in [1] and [7] that substantial improvements in image quality can be achieved in the very close near field through the use of time-domain compensation in continuous wave (CW) imaging systems. The only drawback of this technique, currently known as automatic focusing technique (AFT) [8] is that it requires sophisticated hardware and a considerable amount of data processing, which could be time consuming particularly if implemented in real-time imaging systems. In this paper, it is shown that, when the scanned-frequency signals are sent simultaneously in a broad band pulse, the focusing capabilities of the AFT are maintained. In addition, substantial reduction in signal processing, originally required by the AFT, is obtained. The method presented here, although simple in its nature, is unique in that it uses broad band pulses that can be shaped to meet a prescribed design criteria and produces a true 3-D image.

Manuscript received May 24, 1996; accepted November 15, 1996.

A. Yamani is with the King Fahd University of Petroleum and Minerals, Dahran, Saudi Arabia (e-mail: yamani@ccse.kfupm.edu.sa).

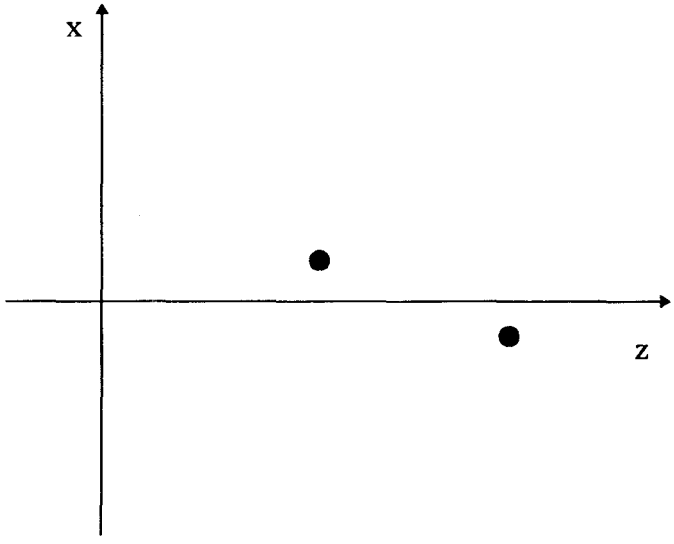

Fig. 1. Geometrical configuration of one-dimensional imaging system.

II. Theory

The multi-frequency automatic focusing technique (MF-AFT) will be briefly presented in this section and shown to be simplified to obtain a new reconstruction procedure, which in this paper is called time-domain automatic focusing technique (TD-AFT). The theory presented here assumes that the data is collected using a series of measurements from a "point-like" sensor. Such sensor might consist of an array of omnidirectional transducers or a single transducer scanned over a planar receiver aperture.

A. Multifrequency Automatic Focusing Technique

The MF-AFT to be described is based upon a mathematical analysis technique, known as angular spectrum decomposition [9]. Data is recorded over a range of frequencies within the bandwidth of a typical transducer, and the method can be applied in circumstances where the defect lies in the very close near field of the recording aperture.

Let $U(x, y, 0; f)$ represent the complex (real and imaginary) acoustic pressure field measured over a 2-D aperture at the plane $z = 0$ and the frequency f is scanned over the transducer bandwidth. By 2-D Fourier transformation with respect

to the spatial coordinates x and y, this pressure field can be represented by its angular spectrum

$$A(s_x, s_y, 0; f) = \int_{-\infty}^{\infty} U(x, y, 0; f) \exp\left[-i2\pi\left(xs_x + ys_y\right)\right] dxdy \quad (1)$$

where s_x and s_y are the spatial frequencies. The angular spectrum of a complex pressure field measured at the plane $z = 0$ is related to that at any other plane z by [9]:

$$A(s_x, s_y, 0; f) = A(s_x, s_y, z; f) B(s_x, s_y, z; f) \quad (2)$$

where

$$B(s_x, s_y, z; f) = \exp(i2\pi f z n C/v), \quad C = \sqrt{1 - (s_x v/nf)^2 - (s_y v/nf)^2}, v \quad (3)$$

is the phase velocity of the wave, and n is an integer equal to 1 for a fixed transmitter-scanned receiver and equal to 2 for a simultaneously scanned transmitter/receiver [1]. If a target is located at a distance z from the receiver aperture, then (2) represents the basis of a multifrequency backward wave propagation imaging scheme. The angular spectrum of the received complex acoustic pressure field can be backpropagated to the target plane by multiplying (2) by the backpropagator filter $B^{-1}(s_x, s_y, z; f)$ to yield an in-focus target image in the spatial frequency domain. It is interesting to note that Busse [10] has viewed (2) as a series of images in the spatial frequency domain at different frequencies. By averaging them over all the frequencies present, and after the application of 2-D inverse Fourier transformation, he [10] obtained high quality images as compared to the single frequency reconstruction algorithm traditionally used in CW imaging systems. However, this elegant approach not only requires a prior target range information z, but it also fails to produce in-focus images of a 3-D target whose dimension in the z-direction exceeds the DOF. In addition, undesirable distortions inherent in the backward wave propagation algorithm [7] can further complicate any diagnostic process. This problem has been completely solved by the MF-AFT [1] as follows: (2) is transformed to the time-domain through the use of a 1-D inverse Fourier transformation with respect to f. As focusing is sensitive to phase only, amplitude variation of the angular spectrum over the transducer bandwidth does not affect the definition of the image (it rather affects its resolution, as will be seen in the simulation part). Furthermore, the variation of the amplitude spectrum over the transducer bandwidth can, in practice, be corrected using known techniques such as equalization or probe compensation. For this, the time-domain angular spectrum of a target can be expressed for simplicity as:

$$A(s_x, s_y, 0; t) \quad \propto \quad B(s_x, s_y, z; t). \quad (4)$$

In theory, it is not possible to obtain an analytical expression of (4) in order to compensate for the nonlinear phase responsible for defocusing the target image. However, a plot of the phase of the angular spectrum $A(s_x, s_y, 0; f)$ with respect to f suggests that this phase can be linearized [7] over the transducer bandwidth and, therefore, an approximate analytical expression of (4) can be derived. Then after, a compensation of the form

$$B'(s_x, s_y; t) = \exp\left[j\left(\phi(s_x, s_y)\, t\right]\right.$$

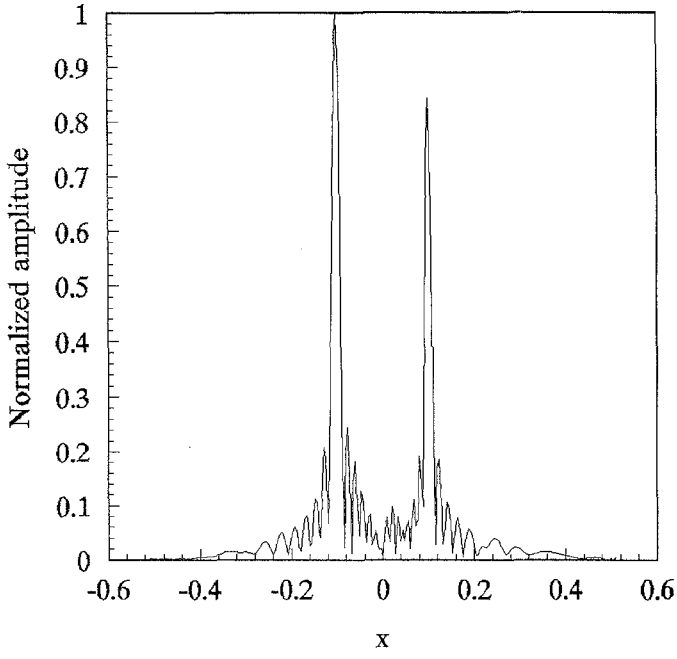

Fig. 2. Image of two-point reflectors at $z_1 = 0.6$ m and $z_2 - 1.2$ m.

is applied to (4) such that once the result is transformed back to the frequency-domain (as required by the MF-AFT algorithm), the center frequency component of the angular spectrum must have a phase equal to 0 mod 2π. This yields the new backpropagator given by:

$$B'(s_x, s_y; t) = \exp\left[-i2\pi f_0 t\left(1 - (s_x\lambda_0/n)^2 - (s_y\lambda_0/n)^2\right)\right] \quad (5)$$

where f_0 and λ_0 are the frequency and the wavelength, respectively, at the center of the transducer bandwidth. Notice that (5) does not contain the radical sign traditionally found in the backpropagator used in conventional CW imaging techniques. It is shown [1] that, when the new backpropagator of (5) is used, in-focus 3-D image is obtained regardless of the axial dimension of the target(s). It is worth noting here that the linearization process of the phase of the angular spectrum $A(s_x, s_y, 0; f)$ is not part of the MF-AFT algorithm, but it was used solely to derive the expression of the new backpropagator given in (5). To summarize, the MF-AFT algorithm consists of the following steps:

1. At each point of the receiver aperture, measure the complex pressure field for each frequency within the transducer bandwidth to obtain $U(x, y, f)$.
2. At each point of the receiver aperture, apply a 1-D inverse fast Fourier transform (IFFT) with respect to f.
3. Apply a 2-D FFT with respect to x and y to obtain the time-domain angular spectrum $A(s_x, s_y; t)$.
4. Apply the backpropagator as in (5).
5. At each spatial frequency, apply a 1-D FFT with respect to time to obtain the corrected angular spectrum $A'(s_x, s_y; f)$.
6. Select the center frequency of the corrected angular spectrum $A'(s_x, s_y; f_0)$.
7. Apply an inverse 2-D FFT with respect to s_x and s_y, and take the square of the magnitude of the resultant data to form an in-focus image.

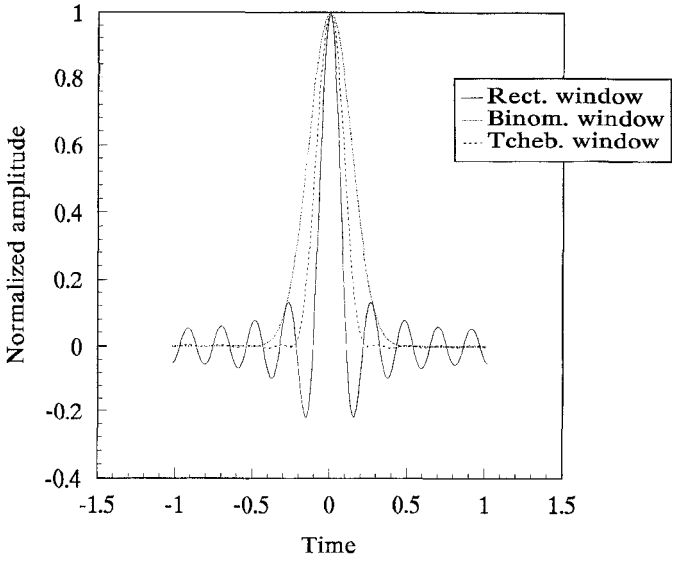

Fig. 3. Pulse envelope for different window functions.

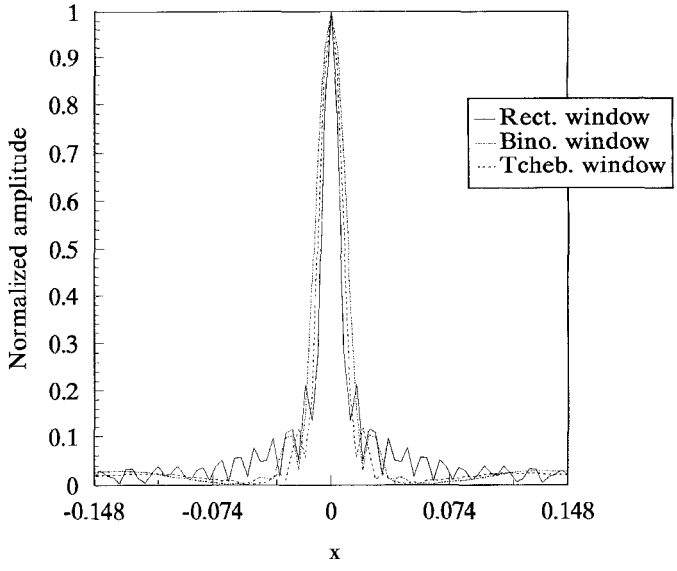

Fig. 4. Effect of weighting on the image of a point-reflector.

B. Time-domain Automatic Focusing Technique

The MF-AFT has proven its focusing capability experimentally in long wavelength imaging systems [7]. However, it requires a considerable amount of data acquisition and processing, which can be time consuming, especially if it is to be implemented in real-time imaging systems. The MF-AFT procedure can be greatly improved by transmitting simultaneously all the scanned-frequency signals in one RF pulse $s(t)$ say, such that the output of the inverse FFT processor in step 2 above, at a given point (x, y) in the receiver aperture, is identical to the complex waveforms recorded at the same position when $s(t)$ is transmitted, i.e.:

$$S(x, y, 0; t) = \int_{-\infty}^{\infty} U(x, y, 0; f) \exp(i2\pi f t)\, df \tag{6}$$

where $S(x, y, 0; t)$ represents a set of complex waveforms recorded by a "point-like" sensor as it is scanned in the plane located at $z = 0$. Steps 3 to 7 are kept unchanged and are used to get in-focus imagery, and the reconstruction procedure hence obtained is called time-domain automatic focusing technique (TD-AFT). Before proceeding further, it is worth mentioning here that the idea of transmitting a pulse $s(t)$ instead of the scanned-frequency signals is simple in its nature but it revolutionizes the MF-AFT and makes it amenable to real-time implementation with a low cost. At this point it can be said that if the "point-like" sensor is scanned in an $N \times N$ positions matrix, then N^2 FFT's are gained. In addition, the sophisticated hardware required to perform the frequency scanning is no longer needed for this new procedure.

To derive the transmitted pulse $s(t)$ needed in the TD-AFT, consider the case where data is recorded over a range of frequencies within the transducer bandwidth. For simplicity, a one-dimensional situation is taken and, in accordance with most practical circumstances, a transmit/receive unit is utilized in the data acquisition plane. The complex acoustic pressure field measured at the ith position in the aperture is given by:

$$U(x_i, 0; f) = U(x_i; f) = rect\left[\frac{f - f_0}{\Delta f}\right] \exp(i4\pi f R_i / v) \tag{7}$$

where Δf is the transducer bandwidth, and R_i is the distance between the target and the ith position of the sensor and is given by:

$$R_i = \sqrt{(x_i - x_t)^2 + z_t^2}$$

and x_t and z_t are the target coordinates. The scanned frequency f is actually a discrete variable defined by:

$$f = f_k = f_0 + k.\delta f$$

where δf is the frequency sampling interval, and k is the frequency index. Thus, the inverse Fourier transform of (7) becomes periodic in the "range-domain" with a period R_m related to δf by:

$$R_m = \frac{v}{2\delta f}. \tag{8}$$

It can easily be shown that the complex envelope of the RF pulse received at the ith aperture position and whose Fourier transform is given by (7) is:

$$S(x_i, R) = 2\delta f \frac{\sin\left[\frac{M\pi}{R_m}(R - R_i)\right]}{\sin\left[\frac{\pi}{R_m}(R - R_i)\right]} \exp\left(-j\frac{4\pi R_i}{\lambda_0}\right) \tag{9}$$

where M is the number of frequencies scanned, and $R = vt/2$ denotes the variable in the range-domain. Equation (9) cannot easily be synthesized in its present form; however, its periodic nature permits its Fourier series expansion to determine the harmonics content of the received pulse. Upon applying the Fourier series expansion of (9), we obtain

$$S(x_i, R) = 2\delta f \left[1 + 2\sum_{n=1}^{(M-1)/2} \cos\frac{2\pi n}{R_m}(R - R_i)\right] \times \exp\left(-j\frac{4\pi R_i}{\lambda_0}\right). \tag{10}$$

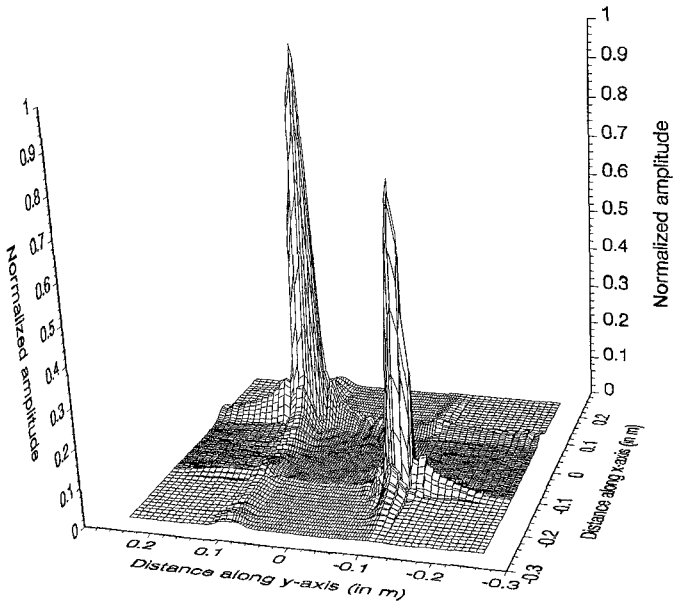

Fig. 5. 3-D image of two point-targets at $z_1 = 0.6$ m and $z_2 = 1.2$ m when a binomial window is applied.

Using (9) and (10) and omitting the phase terms (terms containing R_i) introduced by the propagation paths, and referenced to the time at which the transmitter is fired, the normalized envelope of the transmitted RF pulse can thus be found as:

$$\widehat{s}(R) = \frac{\sin\left(\frac{M\pi R}{R_m}\right)}{\sin\left(\frac{\pi R}{R_m}\right)} = 1 + 2\sum_{n=1}^{(M-1)/2} \cos\left(\frac{2\pi n R}{R_m}\right) \tag{11}$$

It can be seen that the right hand side of (11) can easily now be incorporated in a programmable function generator to synthesize the transmitted RF pulse $s(t)$. In addition, it can be seen from (7) and (11) that the amplitude of each scanned or synthesized frequency component is unity as expected from the rectangular window function used in (7). An appropriate window function with a better figure of merit [11] can be used in the synthesis process to reduce the speckles in the ultrasonic image obtained from TD-AFT. The right-hand side of (11) can thus be rewritten as:

$$\hat{s}(R) = \sum_{n=1}^{(M+1)/2} p_n b_n \cos\left[2\pi\left(n-1\right)\frac{R}{R_m}\right] \tag{12}$$

where $p_n = 1$ for $n = 1$ and $p_n = 2$ otherwise, and b_n represent the weights applied to the pulse. Rectangular (REC), Dolph-Chebyshev (DCB), and binomial (BIN) are among the different types of window functions that are used to weight the harmonics of the broad band pulse in order to investigate the effect of these weights on the quality of the resultant image.

III. Simulations

In this section, the TD-AFT procedure as described in this paper is tested using simulated data. Fig. 1 shows the configuration of a one-dimensional imaging system operating in air at a wavelength $\lambda = 8$ mm, where two point targets are located

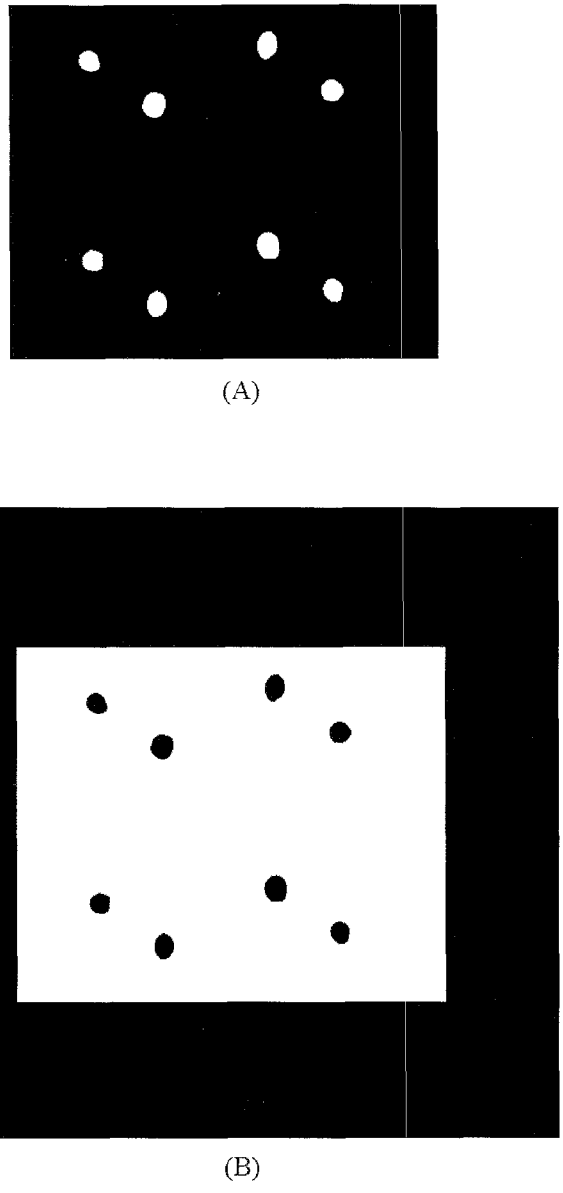

(A)

(B)

Fig. 6. 3-D image of a cube: (A) actual image, (B) inverse contrasted image.

at 75 λ and 150 λ from a 37 λ transmit-receive aperture sampled at $\lambda/2$. Each target is displaced from the central axis by 12.5 λ. The near field of this imaging system is found to extend up to a range of 684.5 λ. In the MF-AFT reconstruction algorithm, a bandwidth $\Delta f = 0.05 f_0$ with $M = 21$ scanned-frequencies (corresponding to a maximum range $R_m = 200\lambda$) is used, whereas in the TD-AFT procedure, 10 harmonics plus D.C. $((M+1)/2)$ are needed to generate the required pulse. The equivalence of the AFT procedures has been tested first, and it has been found that the image (not shown) obtained from the MF-AFT procedure is identical to its counterpart image obtained from the TD-AFT, which is shown in Fig. 2. The dependance of the image spatial bandwidth on the target range [1] is manifested by the difference in the image main beam amplitudes. Next, we will investigate the effect of shaping the pulse on the resultant image. It is well known that the application of a suitable window function [11] in the *frequency domain* reduces the unwanted fluctuations in the *time domain* known as

Gibb's effect in filter design, side lobes in antenna arrays design, and speckles in imaging systems. In our case, the side lobes in the pulse envelope will introduce phase reversal of the carrier signal and may cause a "destructive" interaction between the spatial frequency components, which will lead to increased speckles in the resultant image. Reduction of side lobe levels of the pulse envelope will certainly enhance the quality of the image obtained from the TD-AFT. Fig. 3 shows the effect of the window functions on the pulse envelope. It can be seen that the DCB window function reduces the pulse side lobe levels considerably with minimum widening of the pulse envelope main beam. The effect of these windows on the image is clearly illustrated in Fig. 4 where an on-axis point scatterer located a distance of 64 λ from a transmit-receive aperture is considered. The resultant image witnesses a drop in side lobe level between 5 and 6 dBs from the original level of the first side lobe of the image before weighting is applied. For comparison, the target configuration shown in Fig. 1 is examined using a two-dimensional ($37\lambda \times 37\lambda$) transmit-receive aperture with a DCB window function applied to weight the pulse and the corresponding in-focus image is shown in Fig. 5.

Finally, the case of a three-dimensional target consisting of eight point scatterers, each located at the corner of a cube of 25λ side, is considered. For this test, the center of the cube was located on the z-axis at 110 λ from a $37\lambda \times 37\lambda$ transmit-receive aperture, with two faces initially parallel to the aperture. The cube is then rotated by 25° and 15° about the y and x axes, respectively. Again, 10 harmonics plus D.C. pulse weighted with a DCB window function is used to reconstruct the in-focus image shown in Fig. 6, where it can be seen that simultaneous in-focus image of the point-scatterers is obtained. For clarity, the same image is shown in its inverse-contrast form.

IV. Conclusion

In this paper, it is shown that the drawbacks of the MF-AFT have been eased considerably. The technique is inherently single frequency but uses a broad band pulse for the data acquisition and processing to produce high quality three-dimensional images. In addition, it has been shown that the quality of these images can be further improved by appropriately weighting the harmonics of the pulse. Simulation results are included to validate this technique.

References

[1] A. Yamani, "Depth of field improvements and automatic focusing technique in long wavelength imaging systems," Ph.D. dissertation, Electrical and Electronic Eng. Dept., Sheffield Univ., Sheffield, UK, 1984.

[2] P. D. Corl and G. S. Kino, "A real-time synthetic aperture imaging system," in *Acoustical Imaging*, vol. 9, K. Y. Wang, Ed. New York: Plenum, 1980, pp. 341–355.

[3] G. S. Kino, P. D. Corl, S. Bennett, and K. Peterson, "Real-time synthetic aperture imaging system," in *IEEE Ultrason. Symp. Proc.*, Boston MA, Nov. 1980, pp. 722–731.

[4] T. E. Hall, L. D. Reid, and S. R. Doctor, "SAFT-UT (synthetic aperture focusing technique for ultrasonic testing) real-time inspection system: Operational principles and implementation," 1988.

[5] Y. Ozaki, H. Sumitani, T. Tomoda, and M. Tanaka, "A new system for real-time synthetic aperture ultrasonic imaging," *IEEE Trans. Ultrason., Ferroelect., Freq. Contr.*, vol. 35, pp. 828–838, 1988.

[6] K. Nagai, "A new synthetic aperture focusing method for ultrasonic B-scan imaging by Fourier transform," *IEEE Trans. Sonics Ultrason.*, vol. SU-32, p. 531, 1985.

[7] A. Yamani and J. C. Bennett, "Depth of field improvements and removal of distortion in long wavelength imaging systems," *Proc. Int. Electr. Eng.*, Pt. F, vol. 132, no. 3, June 1985, pp. 149–152.

[8] A. Yamani and M. Hamiane, "Removal of the finite-distance source effect on the applebaum array," *IEEE Trans. Antennas Propagat.*, vol. 41, pp. 1038–1044, Aug. 1993.

[9] J. W. Goodman, *Introduction to Fourier Optics*, New York: McGraw-Hill, 1968.

[10] L. J. Busse, "Three-dimensional imaging using a frequency-domain synthetic aperture focusing technique," *IEEE Trans. Ultrason., Ferroelect., Freq. Contr.*, vol. 39, pp. 174–179, Mar. 1992.

[11] F. J. Harris, "On the use of windows for harmonic analysis with the discrete Fourier transform," *IEEE Proc.*, vol. 66, pp. 51–83, Jan. 1978.